Supporting Information

Shrestha et al. 10.1073/pnas.1404264111

SI Materials and Methods

Mice. Tuberous sclerosis 1 floxed alleles (*Tsc1*$^{fl/fl}$), CD45.1, and T-cell receptor-transgenic OT-I mice were purchased from the Jackson Laboratory. *Bcl2*-transgenic and *Rosa26*–Cre–ER^{T2} (CreER) mice have been described previously (1). Cre recombinase under control of the Granzyme B promoter (*GzmB*–Cre) mice were kindly provided by J. Jacob (Emory University, Atlanta) and M. Li (Memorial Sloan Kettering Cancer Center, New York). All mice have been backcrossed to the C57BL/6 background for at least eight generations, with *Tsc1*$^{fl/fl}$ littermates used as the WT control mice. Animal protocols were approved by the Institutional Animal Care and Use Committee of St. Jude Children's Research Hospital.

***Listeria monocytogenes* Infection.** For the study of primary immune response, mice were i.v. infected with 3×10^4 colony-forming units (cfus) of *Listeria monocytogenes* expressing the chicken ovalbumin (LM–OVA). For the analysis of secondary immune response, mice were rechallenged with 5×10^4 cfu of LM–OVA at day 35 or more after primary infection. The recall responses were determined 4–6 d after the secondary infection.

Flow Cytometry. For analysis of surface markers, cells were stained in PBS containing 2% (wt/vol) BSA, with anti-CD4 (RM4-5), anti-CD8α (53-6.7), anti-TCRβ (H57-597), anti-CD44 (1M7), anti-CD62L (MEL-14), anti-KLRG1 (2F1), anti-CD127 (A7R34), anti-CD45.1 (A20), anti-CD45.2 (104), anti-CD244.2 (eBio244F4) (eBioscience), and Tim-3 (215008) (R&D Systems). The OVA peptide [comprised of amino acids Ser-Ile-Ile-Asn-Phe-Glu-Lys-Leu (SIINFEKL)]-loaded mouse H-2K^b tetramer was from the Baylor Tetramer Production Facility. For in vivo BrdU labeling, mice were injected intraperitoneally with BrdU (1 mg) and analyzed 16 h later according to the manufacturer's instructions (BD Biosciences; 552598). Caspase-3 staining was performed according to the manufacturer's instructions (BD Biosciences). For intracellular staining, anti-Eomes (Dan11mag), anti–CTLA-4 (UC10-4B9), and anti–K_i-67 (20Raj1) were purchased from eBioscience; anti–T-bet (4B10) and anti-Gzmb (GB11) from Biolegend; anti-Bcl2 (N46-467) from BD Biosciences; and anti–Blimp-1 (3H2-E8) from Thermo Scientific. For intracellular cytokine staining, CD8$^+$ T cells were stimulated for 5 h with $OVA_{257–264}$ (SIINFEKL) in the presence of monensin before being stained according to the manufacturer's instructions (BD Biosciences). ROS production was measured by incubating T cells for 30 min at 37 °C with 10 μM 5-(and-6)-chloromethyl-2,7-dichlorodihydrofluorescein diacetate acetyl ester (Invitrogen) after staining of surface markers. Staining with antibodies to S6 phosphorylated at Ser235 and Ser236 (D57.2.2E; Cell Signaling Technology) was done after fixing cells with Phospho Lyse/Fix Buffer, followed by permeabilization with Phosflow Perm Buffer III (BD Biosciences). Flow cytometry data were acquired on an LSRII or LSR Fortessa (BD Biosciences) and analyzed with FlowJo software (TreeStar).

Cell Purification and Culture. Sorted naïve T cells (CD8$^+$CD62L^{hi} CD44^{lo}) from OT-1$^+$ *Tsc1*$^{+/+}$ CreER$^+$ and OT-1$^+$ *Tsc1*$^{fl/fl}$ CreER$^+$ mice were cultured in vitro in Click's medium (plus β-mercaptoethanol) supplemented with 10% (vol/vol) FBS and 1% (vol/vol) penicillin–streptomycin and stimulated with 10 μg/mL SIINFEKL peptide and 100 U/mL IL-2 for 4 d in the presence of 0.5 μM 4-hydroxytamoxifen (4-OHT). Ficoll-purified live CD8$^+$ T cells were then stimulated with IL-15 (50 ng/mL) or IL-2 (50 U/mL) in the presence of rapamycin (50 nM) or mock.

Cell Isolation and Adoptive Transfer. For adoptive transfer, naïve CD8$^+$ T cells from OT-I$^+$ (CD45.2$^+$) and *Tsc1*$^{-/-}$OT-I$^+$ (CD45.1.2$^+$) were transferred to CD45.1$^+$ recipients. One day after transfer, mice were infected with 3×10^4 cfu of LM–OVA for the primary response and 5×10^4 cfu of LM–OVA for the recall response. OVA$^+$ CD8$^+$ T cells were sorted from the spleen of WT or *Tsc1*$^{-/-}$ mice (CD45.2$^+$) at day 41 p.i. and transferred into congenically marked (CD45.1$^+$) recipients. One day after the transfer, mice were infected with 5×10^4 cfu of LM–OVA and used for the analysis of secondary CD8$^+$ T-cell responses at days 4–6.

Metabolic Assay. The bioenergetic activities of the extracellular acidification rate and oxygen consumption rate pathways were measured using the Seahorse XF24-3 Extracellular Flux Analyzer per the manufacturer's instructions (Seahorse Bioscience). The glycolytic flux assay was determined by measuring the detritiation of [3-^{3}H]-glucose, as described (2).

Gene Expression Profiling by Microarray Analysis. RNA samples from freshly isolated OVA$^+$ CD8$^+$ cells from WT ($n = 4$ after the exclusion of one sample due to abnormal GAPDH 3′/5′ ratio and based on principal component analysis) and *Tsc1*$^{-/-}$ mice ($n = 5$) were analyzed with the Affymetrix HT MG-430 PM GeneTitan peg array, and expression signals were summarized with the robust multiarray average algorithm (Affymetrix Expression Console v1.1). Lists of differentially expressed genes by ANOVA [false discovery rate (FDR) < 0.1] were analyzed for functional enrichment using the Ingenuity Pathways (www.ingenuity.com). GSEA within canonical pathways was performed as described (3).

RNA, Genomic DNA, and Immunoblot Analyses. Real-time PCR analysis was performed with primers and probe sets from Applied Biosystems, as described (4). Genomic DNA (gDNA) was purified from the sorted naïve CD8$^+$ (CD8$^+$CD62L^{hi}CD44^{lo}) T cells using a DNeasy blood and tissue kit from Qiagen. Tsc1 gDNA was quantified by real-time PCR normalizing with nuclear intron of β-globin gDNA with the following primers: Tsc1 forward 5′-GTCACGACCGTAGGAGAAGC-3′, Tsc1 reverse 5′-GAATCAACCCCACAGAGCAT-3′, and β-globin forward 5′-GAAGCGATTCTAGGGAGCAG-3′, β-globin reverse 5′-GGAGCAGCGATTCTGAGTAGA-3′. Immunoblots were performed as described previously (5), using the following antibodies: p-S6 (2F9; Cell Signaling Technology) and β-actin (AC-15; Sigma).

Statistical Analysis. *P* values were calculated with Student *t* test (GraphPad Prism). *P* values of less than 0.05 were considered significant. All error bars represent the SEM.

1. Yang K, Neale G, Green DR, He W, Chi H (2011) The tumor suppressor Tsc1 enforces quiescence of naive T cells to promote immune homeostasis and function. *Nat Immunol* 12(9):888–897.
2. Shi LZ, et al. (2011) HIF1alpha-dependent glycolytic pathway orchestrates a metabolic checkpoint for the differentiation of TH17 and Treg cells. *J Exp Med* 208(7):1367–1376.
3. Subramanian A, et al. (2005) Gene set enrichment analysis: A knowledge-based approach for interpreting genome-wide expression profiles. *Proc Natl Acad Sci USA* 102(43):15545–15550.
4. Liu G, et al. (2009) The receptor S1P1 overrides regulatory T cell-mediated immune suppression through Akt-mTOR. *Nat Immunol* 10(7):769–777.
5. Liu G, Yang K, Burns S, Shrestha S, Chi H (2010) The S1P(1)-mTOR axis directs the reciprocal differentiation of T(H)1 and T(reg) cells. *Nat Immunol* 11(11):1047–1056.

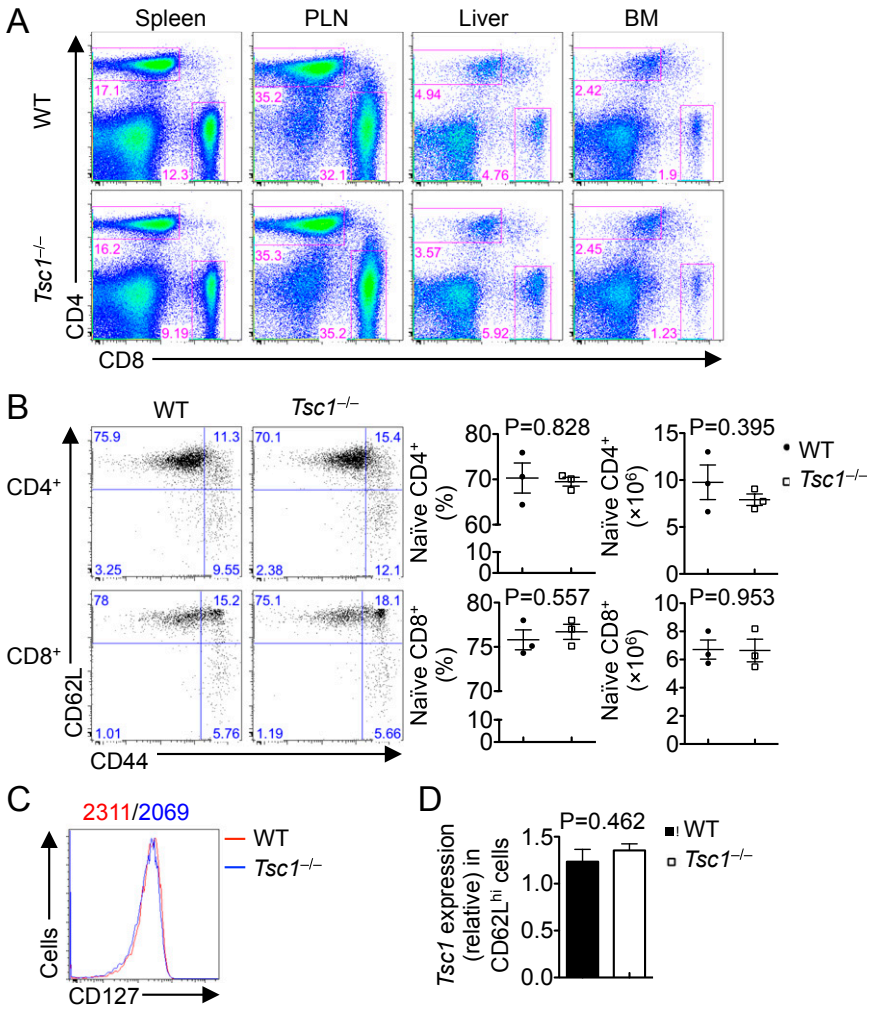

Fig. S1. Normal homeostasis of CD4$^+$ and CD8$^+$ T cells in *Tsc1*$^{-/-}$ mice under steady state. (*A*) Flow cytometry of conventional T cells in the spleen, peripheral lymph nodes (PLNs), liver, and bone marrow (BM) from WT and *Tsc1*$^{-/-}$ mice. (*B*) Expression of CD62L and CD44 (*Left*) and the frequency (*Center*) and number (*Right*) of naïve CD4$^+$ and CD8$^+$ (CD62L^{hi}CD44^{lo}) T cells. (*C*) Expression of CD127 on CD8$^+$ T cells from WT and *Tsc1*$^{-/-}$ mice. (*D*) Real-time PCR analysis of *Tsc1* mRNA expression in naïve CD8$^+$ (CD62L^{hi}CD44^{lo}) T cells from WT and *Tsc1*$^{-/-}$ mice. Data are representative of two independent experiments and are presented as the mean ± SEM.

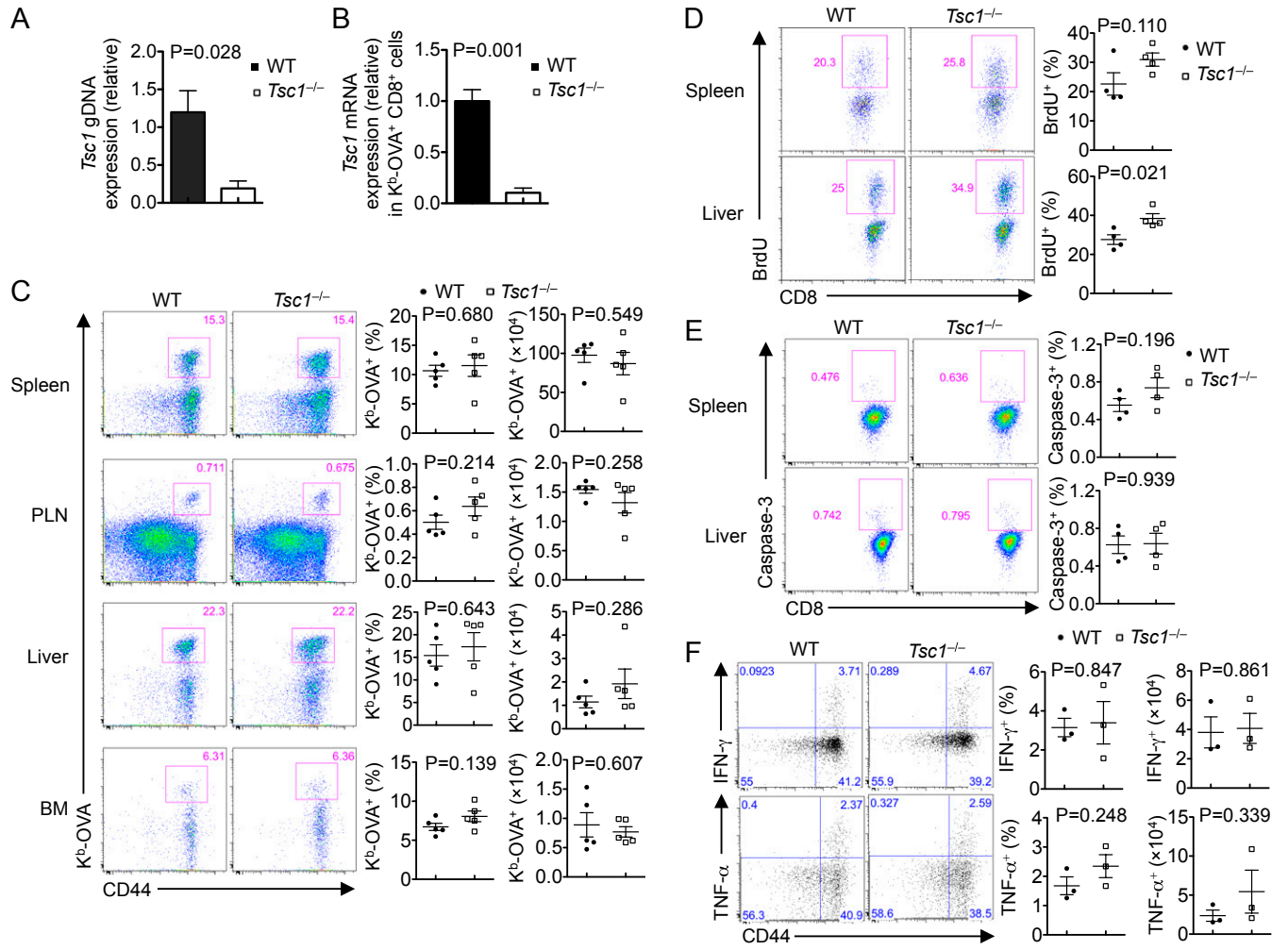

Fig. S2. Tsc1 deficiency does not impact the effector response of CD8$^+$ T cells. WT and *Tsc1*$^{-/-}$ mice were infected with LM–OVA and analyzed at day 9 p.i. (*A* and *B*) Real-time PCR analysis of *Tsc1* gDNA (*A*) and mRNA expression (*B*) in K^b-OVA$^+$ CD8$^+$ T cells at day 9 p.i. (*C*) Representative flow cytometry plots of CD8$^+$ T cells (*Left*) and the frequency (*Center*) and number (*Right*) of K^b-OVA$^+$ CD8$^+$ T cells. (*D*) BrdU staining of K^b-OVA$^+$ CD8$^+$ T cells in the spleen and liver of WT and *Tsc1*$^{-/-}$ mice at day 9 p.i. (*Left*) and the frequency of BrdU$^+$ cells (*Right*). (*E*) Caspase-3 staining of K^b-OVA$^+$ CD8$^+$ T cells in the spleen and liver of WT and *Tsc1*$^{-/-}$ mice at day 9 p.i. (*Left*) and the frequency of Caspase-3$^+$ cells (*Right*). (*F*) At day 9 p.i., splenocytes from WT and *Tsc1*$^{-/-}$ mice were restimulated with the SIINFEKL peptide for intracellular cytokine staining of IFN-γ and TNF-α. Shown are representative flow cytometry plots of CD8$^+$ T cells (*Left*) and the frequency (*Center*) and number (*Right*) of IFN-γ$^+$ and TNF-α$^+$ CD8$^+$ T cells. Data are representative of two independent experiments (*B–F*) or one experiment (*A*; $n = 3$ mice per group) and are presented as the mean ± SEM.

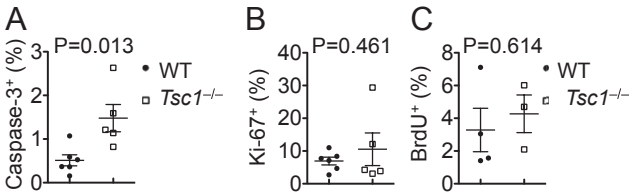

Fig. S3. Proliferation and survival of Tsc1-deficient CD8$^+$ T cells during the contraction phase. Flow cytometry of Caspase-3$^+$ (*A*), K_i-67$^+$ (*B*), and BrdU$^+$ (*C*) in K^b-OVA$^+$ CD8$^+$ T cells in the spleen from WT and *Tsc1*$^{-/-}$ mice at day 18 p.i. Data are representative of two independent experiments and are presented as the mean ± SEM.

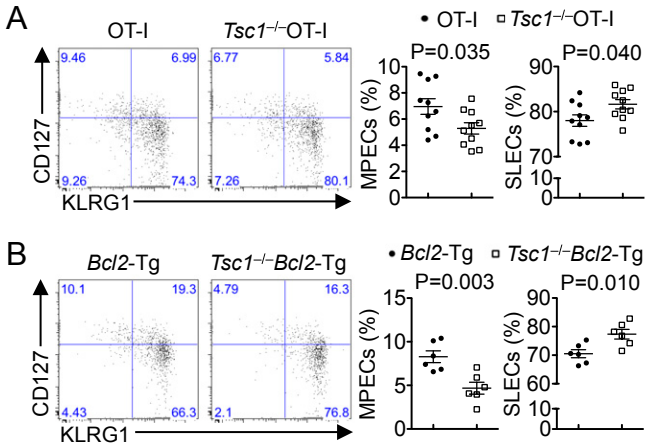

Fig. S4. Intrinsic role of Tsc1 in the differentiation of memory precursors. (*A*) Naïve CD8$^+$ T cells from OT-I$^+$ (CD45.2$^+$) and *Tsc1*$^{-/-}$OT-I$^+$ (CD45.1.2$^+$) mice were isolated, mixed at a 1:1 ratio, and transferred to CD45.1$^+$ recipients, followed by LM–OVA infection 1 d later. Flow cytometry of CD127 and KLRG1 expression and frequencies of memory-precursor effector cells (MPECs) and short-lived effector cells (SLECs) from OT-I$^+$ (CD45.2$^+$) and *Tsc1*$^{-/-}$OT-I$^+$ (CD45.1.2$^+$) donor T cells out of the total K^b-OVA$^+$ CD8$^+$ T cells at day 7 p.i. (*B*) Flow cytometry of CD127 and KLRG1 and frequencies of MPECs and SLECs in K^b-OVA$^+$ CD8$^+$ T cells from *Bcl2*-transgenic (Tg) and *Tsc1*$^{-/-}$*Bcl2*-Tg mice at day 8 p.i. Data are representative of two independent experiments and are presented as the mean ± SEM.

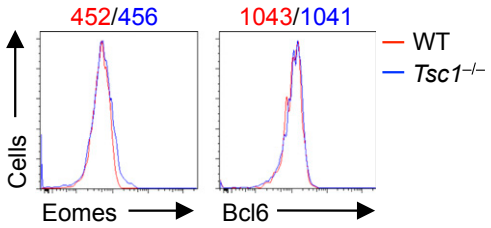

Fig. S5. Expression of transcription factors implicated in memory T-cell differentiation. Intracellular staining of Eomes and Bcl6 in splenic K^b-OVA$^+$ CD8$^+$ T cells from WT and *Tsc1*$^{-/-}$ mice at day 9 p.i. Data are representative of three independent experiments.

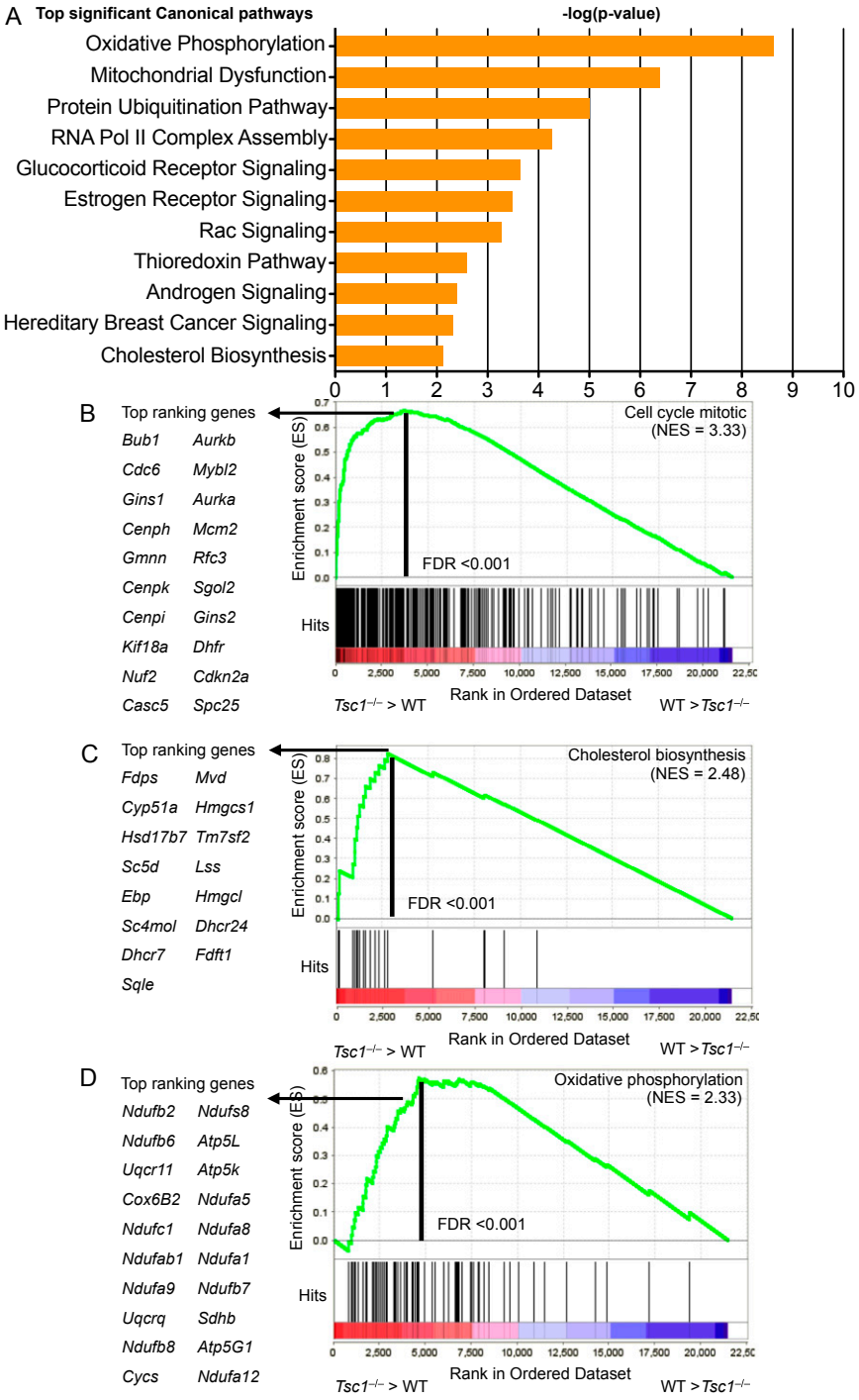

Fig. S6. Dysregulated cell metabolism in Tsc1-deficient T cells. (*A*) Ingenuity pathway analysis of canonical pathways controlled by Tsc1 in K^b-OVA^+ $CD8^+$ T cells sorted from mice at day 9 p.i. (FDR < 0.1). (*B–D*) GSEA reveals the overrepresentation of signature genes in cell-cycle mitotic (*B*), cholesterol biosynthesis (*C*), and oxidative phosphorylation (*D*) in Tsc1-deficient $CD8^+$ T cells at day 9 p.i. ($n = 4–5$ mice per genotype). The middle part of the plots shows the distribution of the genes in each gene set ("Hits") against the ranked list of genes. The lists on the left show the top genes in the leading edge subset. NES, normalized enrichment score.

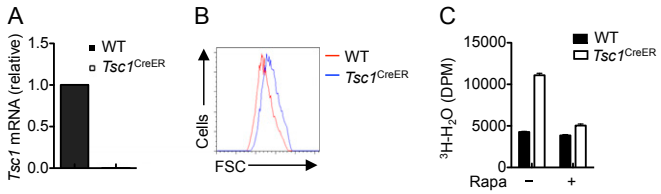

Fig. S7. Tsc1-dependent effects on cell size and glycolytic activity in activated *Tsc1*$^{fl/fl}$ CreER^{+} OT-I^{+} cells upon 4-OHT treatment. Naïve CD8^{+} T cells from *Tsc1*$^{+/+}$ CreER^{+} OT-I^{+} (WT) and *Tsc1*$^{fl/fl}$ CreER^{+} OT-I^{+} (*Tsc1*^{CreER}) mice were stimulated with OVA in the presence of IL-2 and 4-OHT for 4 d, followed by analysis of *Tsc1* mRNA expression (*A*), cell size (*B*), and glycolytic activity after IL-15 stimulation for 24 h in the absence or presence of rapamycin (Rapa) (*C*). Data are representative of two independent experiments.

Other Supporting Information Files

Dataset S1 (XLSX)